

# **The Effectiveness of a 3D Printed Hydrogel Membrane to Sustain Algal Growth**

Ben Caroway, Satchel Malo, and Frank Parsons

## Abstract

This research demonstrates the potential of a photosynthetic algae—*chlorella vulgaris*—to grow within *carrageenan hydrogel*, an inexpensive and sustainable material that would enable industrial scale fabrication of algae biofilters. Photosynthetic algae are well suited for pollutant removal applications, primarily due to their tolerance of toxic environments. They are also significant for bioremediation because they can convert both airborne and aqueous pollutants into biomass. For example, their photosynthetic functions are used to convert carbon dioxide (CO<sub>2</sub>) into oxygen and biomass. As for aqueous pollutants, algae can capture products of agricultural runoff such as nitrates and nitrites. While this often leads to an algal bloom that can negatively impact aquatic environments, a controlled algae population could also be beneficial for regulating such pollutants. Choosing a proper material for regulated algal growth can be problematic as the amount of nutrients, space, and pollutants need to be balanced in order for the culture to thrive. One possible material is carrageenan hydrogel, a linear sulfated polysaccharide derived from red seaweed. Carrageenan hydrogel was selected for this study because of its low toxicity and remarkable structural properties. The long carrageenan polymer chains formed through gelation allow the material to be formed into almost any 3-dimensional (3D) structure. This makes it an ideal substance for additive manufacturing (3D printing). In this study, a rudimentary desktop 3D printer and newly developed pneumatic pump system aided in the extrusion of carrageenan hydrogel. By 3D printing the material, novel biofilter designs can be more easily prototyped. This study investigated the ability of algae to grow in unmodified hydrogel material, which can help in establishing future improvements that could make the gel more biocompatible.

## Introduction

Over the past decade, global energy demands have been rising. With slow progress in the development of renewable technologies, humanity has developed a reliance on quick burning fossil fuels such as coal, oil and natural gas. These combustion fuel sources have intensified the release of greenhouse gases. In 2018, international carbon dioxide (CO<sub>2</sub>) emissions reached a record high of 33.1 gigatons (Gt), a 1.7% increase from the previous year. This change of about 560 megatons (Mt) is equal to the amount of CO<sub>2</sub> emitted from the airline industry alone (International Energy Agency, 2019). While CO<sub>2</sub> is a common and naturally occurring gas that helps to normalize temperatures in Earth's atmosphere, excessive additions of the substance through human activity have caused uncharacteristic changes in global climate (National Aeronautics and Space Agency, NASA, 2010). CO<sub>2</sub> is constantly cycled throughout the Earth's many biological systems. One way it is exchanged from the atmosphere is through chemical reactions on the ocean's surface which form carbonic acid (H<sub>2</sub>CO<sub>3</sub>); H<sub>2</sub>CO<sub>3</sub> has been steadily decreasing the pH of the ocean from about 8.21 to 8.1 since the dawn of the industrial revolution. This shift in acidity has caused the shells and structures of many coral reefs to dissolve, damaging large portions of Earth's marine life (National Oceanic and Atmospheric Administration, NOAA, 2019). In order to combat serious environmental issues such as ocean acidification, increased regulation of atmospheric pollutants is needed. Despite a societal push to burn cleaner fossil fuels such as natural gas, greenhouse gas emissions have continued to impact the biosphere and degrade human health. Even with the danger of an increasingly contaminated atmosphere, efforts to design an efficient and reliable pollution control system have yet to become successful enough for large scale implementation in power plants. Development of a

universal device for airborne pollutant removal is still unattainable due to a variety of economic hurdles. By balancing material cost, functionality at a large scale, and efficiency, research into air remediation systems can help to improve atmospheric quality while also keeping costs low and feasible for any part of the world (Environmental Protection Agency, EPA, 2019).

One promising technology for the reduction of greenhouse gases is photobioreaction. Using single or multi-celled algae, cyanobacteria, or moss, the process of photosynthesis can be exploited for large scale removal of pollutants such as CO<sub>2</sub>, sulfur dioxide (SO<sub>2</sub>), and nitrogen dioxide (NO<sub>2</sub>, IGV GmbH, 2011). Algae in particular are notable for use in bioreactors because they are efficient at converting CO<sub>2</sub> to biomass and oxygen. They can also be burned for biofuel or used as a food source after pollutant removal (National Cooperative Extension, 2019).

Traditional methods of scrubbing waste air from coal fired power plants involve neutralization of CO<sub>2</sub> and SO<sub>2</sub> through an alkaline sorbent material such as limestone or gypsum. This process has an extremely high efficiency of 90%, however high operating costs of the design make these chemical scrubbers challenging to implement for smaller power plants. In addition to cost, they also produce substantial amounts of waste that can be difficult to sell or recycle (EPA, 2002). For this reason, research into an economical and long term photobioreactor solution is essential for controlling point source pollution. One place where researchers are bridging the gap between the theory and reality of bioreactors is at the East Bend Coal Fired Power Plant in Union, Kentucky. Students at the University of Kentucky have constructed tubular photobioreactors that filter flue gas (CO<sub>2</sub>, SO<sub>2</sub>, NO<sub>2</sub> mix) through aquatic cultures of algae. The primary function of the algae is to convert the harmful flue gas into biomass that can be utilized in other applications. After pollutant absorption rate drops, the algae undergoes a process known as flocculation. During

flocculation, the algae cells stick together in clumps from the addition of a chemical binding agent. The algae colloids eventually become heavy enough to sink to the bottom and can be removed for analysis. This nutrient rich byproduct has a multitude of uses such as in the feed material for livestock and in many kinds of biofuel (University of Kentucky, 2013). When it comes to biofuel, studies have been done to extract lipids and natural oils from algal cells. These oils have a high energy density—even greater than the oils derived from corn. Researchers predict that algae may be able to outperform corn in terms of biofuel production because of their immense genetic diversity. With more than 100,000 unique species available, algae can be custom tailored to biofilters based on the pollutants their species is most effective at removing (U.S. Department of Energy, 2012).

While algae offer an innovative method of bioremediating air, there are still many obstacles to overcome when developing a bioreactor. Algae are more tolerant to pH, nutrients, and light, than other organisms; however these characters of a biofilter still need to be maintained to a certain degree in order to prolong the life of the algae cells. In Europe, bioscrubbers utilizing bacterial cultures have been used to filter volatile compounds (VOCs) such as alcohols and ketones from the air. These systems are functional on the experimental scale, however intense monitoring of the bacteria's liquid media is required because of drastic pH and nutrient fluctuations (Devinney et al, 1999). Similarly, liquid algae cultures also need monitoring because a majority of algal species prefer a pH from neutral to alkaline and saline growing conditions (Clifford, n.d.). Due to the significant maintenance cost of growing commercial amounts of algae, experiments have been done to immobilize the organisms in a biocompatible material, which allows for nutrients to be evenly dispersed among the algal cells,

and provides greater surface area for pollutant accumulation (Gonzalez-Delgado et al, 2016). Most of this immobilization takes place in hydrogel, a hydrophilic polymer composed of roughly 90% water. Hydrogel can be fabricated from a variety of different substances, however alginate and carrageenan are more common for plant-based gels (Jovic et al, 2019). In previous studies, algae cultures have been grown in alginate based hydrogel; results of these studies show that while algae can grow inside the alginate, longevity of the cells heavily depends on gel density and structure (Calvert, 2016). Alginate hydrogel tends to form weak bonds after polymerization, causing algal cells to diffuse in the material and separate from vital nutrients (Jovic et al.). For this reason, carrageenan hydrogel is more appropriate for sustaining a cellular culture due to its longer polymer structure. Also, by introducing nanoscopic silica particles to carrageenan hydrogel, the material becomes thermoreversible, allowing for recycling of the hydrogel. When the material needs to be reshaped or salvaged, heating it weakens hydrogen bonds between the carrageenan and nanosilicates, turning the hydrogel back into its liquid state prior to the cross-linking process (Wilson et al, 2017). The benefits of testing carrageenan hydrogel come from its low cost, biocompatibility and desirable properties for 3D bioprinting.

3D printing of hydrogel is a reliable method for both scalable manufacturing and structural testing. Utilizing 3D printing technology, hydrogel can be shaped into complex structures with high surface area for pollutant accumulation. These hydrogel structures can be quickly developed and modified using software prior to printing, allowing structural models to be edited without human error affecting print quality (Suntornnond et al, 2016). Hardware modifications can also improve the printing of biomaterials. By adding control electronics to a syringe pump, hydrogel extrusion can be finely adjusted based on viscosity and extruder size.

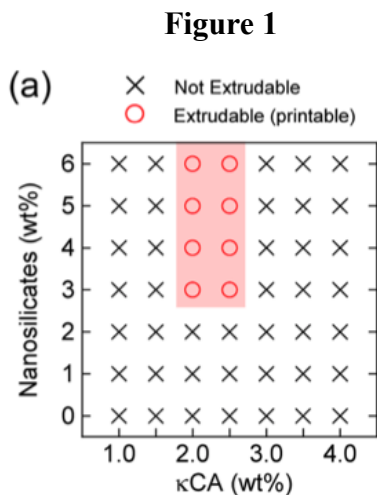
Carrageenan hydrogel as a substance demonstrates great potential for 3D bioprinting (Schaffner et al, 2017), and due to thermo-reversibility, failed prints can be salvaged back into gel mixture. This allows for unstable structures to be created without risk of losing material.

Despite the versatility and low cost of hydrogel, there is little research put into optimizing the compound for printing and practical use. The purpose of this research was to expand upon its use by growing a commonly available algae in carrageenan hydrogel, a highly biocompatible variant that should facilitate algal growth and be extrudable in a desktop 3D printer. It was predicted that the *Chlorella vulgaris* would grow within carrageenan hydrogel because of the material's low toxicity and high surface area.

## Hydrogel Methods

### Hydrogel Mixing and Preparation

For this study, all hydrogel batches were mixed with a magnetic stir bar and heated on a Fisher Scientific 11-100-49SH hotplate. In order to fabricate hydrogel with desirable properties for 3D printing, a known material concentration was used to achieve a similar consistency between each of the gel solutions. These values were based on a chart developed by Wilson et al. (2017, Figure 1).



A material concentration of 2 wt.% kappa carrageenan was combined with 3 wt.% of Laponite RDS, a nanosilica based rheological additive. Laponite RDS is a highly shear thinning layered silicate rheological additive for water-borne systems. Three 300 milliliters (mL) beakers were used to mix separate batches of hydrogel on hotplates. Based on a maximum of 300 mL, the initial volume of every batch was limited to 200 mL.

Previous research suggests that larger hydrogel batches become difficult to heat evenly, causing certain parts of the solution to gel at varying times. For this reason, the mixing process was split between multiple beakers. To begin hydrogel synthesis, 142.5 mL of spring water was measured out into the beakers and placed on the hotplates with magnetic stirring. 4.5 grams (g) of Laponite RDS was added to each beaker and the stirring was set to 350 revolutions per minute (RPM). The nanosilicates were dissolved in the solution for 25 minutes at room temperature and then heated. After 30 Minutes, 3 g of carrageenan was added and the stirring was raised to 700 RPM. Due to this change in mass, the heating rate decreased and the temperature leveled off at around

50 degrees celsius ( $^{\circ}\text{C}$ ), requiring the hotplate to be adjusted to  $190^{\circ}\text{C}$  after 38 minutes. As the solution started to take on a more viscous consistency, higher temperatures and stirring were needed to keep it from gelling. With a target temperature of  $80^{\circ}\text{C}$ , the heating and agitation were increased to 900 RPM at 45 minutes and  $210^{\circ}\text{C}$  at 50 minutes. The first batch to reach the temperature threshold of  $80^{\circ}\text{C}$  was removed and poured into the 200 mL beaker for viscosity testing. This left the remaining beakers to finish heating at  $200^{\circ}\text{C}$ .

The temperature of the gels was measured with Vernier temperature probes connected to a computer running Logger Pro. This measurement of temperature aided in estimating the times to increase the heat setting on each hotplate. For different volumes and types of hydrogel, the heating curve will vary; but based on what was observed in Logger Pro, 200 mL of carrageenan hydrogel is effectively heated and mixed through the procedure in the previous paragraph. The structural quality of a hydrogel tends to increase as it's heated and then starts to decrease with further heat as it breaks down bonds between the carrageenan polymer. Without degrading the polymer or significantly evaporating the solution, it was found that the process of carrageenan hydrogel synthesis takes roughly an hour at small volumes.

### Measuring Hydrogel Properties: Temperature and Viscosity

The heated hydrogel products were characterized with a rotational viscometer. A generic branded NDJ-8S model was chosen to assess how hydrogel viscosity changes overtime with respect to temperature. Following manufacturer recommendations, a narrow 200 mL beaker was used to completely surround the spindle of the viscometer with hydrogel solution. For each test, a gel was removed from its hotplate upon reaching 80°C, and was poured into the 200 mL beaker.

The temperature of the viscometer beaker was tracked with Logger Pro. The NDJ-8S viscometer spindle sizes range from 0 to 4, each with an increasingly wider range of measuring capabilities. The lesser spindle numbers (0 and 1) provide more accurate data for fluids with a viscosity below 60,000 millipascal seconds (mPa·s). For the majority of viscosity tests with hydrogel, spindle number 3 was selected. By adjusting the RPM of the spindle, the number 3 spindle goes from 2,000 mPa·s (60 RPM) to 1,200,000 mPa·s (0.1 RPM). For reference, the viscosity of water is about 1 mPa·s at 20°C. After calibrating the instrument, an RPM of 0.3 provided the most accurate range of data for the relatively high viscosity of hydrogel. Over the series of viscosity tests, it fluctuated between 70,000 and 120,000 mPa·s, falling within the measuring range of 0.3 RPM (0 - 400,000 mPa·s). The viscometer outputs a viscosity reading every 200 seconds. Due to the lengthy time between readings, only 5 were taken per batch. The temperature readings in Logger Pro were written down with the viscosity data for later correlation.

## Algae Methods

### Culturing Algae for Use in Hydrogels

Cultures of photosynthetic algae *Chlorella Vulgaris* were received from Algae Research and Supply. A growth kit came with the algae containing a stock nutrient media and potassium culture salts. The stock media was a modified version of the F/2 formula developed by Guillard and Ryther (1962). The algae was cultured in three 1 liters (L) mason jars filled with spring water. Roughly 50 mL of the nutrient solution along with 10 g of the potassium salts were added



to each jar followed by 50 mL of the algae solution split between them. The jars were then placed under two 30 watt LED grow lights. While the combination of the F/2 media and salts worked well initially, a problem quickly arose where the algae began to clump and turn yellow, dropping to the bottom of the jars. It was identified that the potassium salts were significantly disrupting the pH of water, increasing from about 7 to 12. The purpose of the salts is to

**Figure 2** *Liquid cultures of Chlorella Vulgaris* provide the algae with soluble nutrients in the water and to neutralize an acidic pH. However, the extremes observed in these jars required the use of a different growth medium. A portion of the algae was removed and transferred to new jars with BG11 medium. BG11 is a nutrient media designed for growing cyanobacteria, however it has also been successful with *Chlorella Vulgaris* in the past. The BG11 prolonged the lifespan of each culture, allowing the cells to reproduce gradually instead of blooming and dying off.

### Adding Algae to Hydrogel

Upon culturing the *Chlorella Vulgaris*, it was then prepared for insertion into hydrogel solution. In order for the water and nutrients in the culture to not affect hydrogel consistency, they were removed from the algal cells through centrifugation. 30 mL of culture was pipetted into four test tubes and placed in a Fisher Scientific Marathon 21K centrifuge.

The algae was spun down from solution at 3500 RPM for 10 minutes. After removal from the centrifuge, 25 mL of the wastewater was pipetted off, leaving 5 mL of concentration algae solution. To finally add the algae to hydrogel, the material had to be cooled from 80°C to about 35°C, a temperature slightly below the thermal tolerance of *Chlorella Vulgaris*. The printability of hydrogel is more optimal at higher temperatures because of a lower viscosity. For this reason, an attempt was made to maximize the hydrogel temperature while also staying within the livable range of the algae.



**Figure 3** Concentrated algae solution

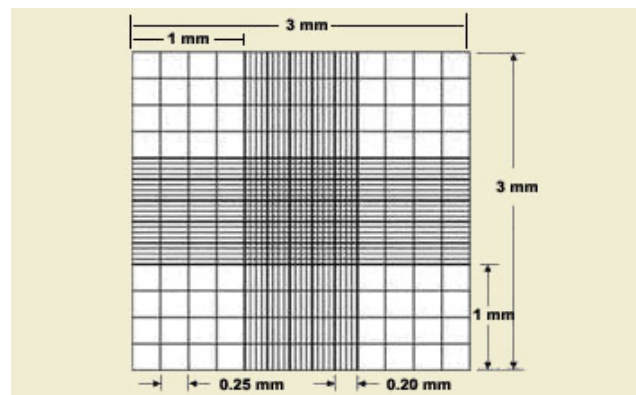
### Quantifying Algal Growth in a Hydrogel Culture

The ability of *Chlorella Vulgaris* to grow within carrageenan hydrogel was thoroughly tested in multiple batches of material over a period of 18 to 30 days. In 5 of those batches, the amount of algal cells was measured before and after addition to the hydrogel. Cell counts were made using a chip hemocytometer and optical microscope. For algae that was grown outside the hydrogel as a control, a  $\frac{1}{3}$  dilution was made to avoid oversaturation of cells on the counting grid. This was completed for both the initial and final samples of algae. For algae grown inside hydrogel, the cells had to be extracted for counting. 10 g of each hydrogel batch was dissolved in 300 mL of spring water through vigorous heating and mixing. Vortexing of the hydrogel samples was also needed to separate clumps of cells. To count cells that grew independent of the hydrogel, a pattern of four small squares (1/400 square millimeters, mm) on the chip was used to estimate concentration. Each sample of algae was counted three times by three different people to reduce bias and obtain a reasonable average. One problem with counting the algae grown in hydrogel was the large dilution made in 300 mL of water. Since this made the distribution of cells much too great to obtain data from the small squares, 10 medium squares (1/25 square mm.) were substituted instead. The math used to derive cell count estimates is listed below with an example.

**Figure 4** Macroscopic view of chip hemocytometer.



**Figure 5** Layout of chip grid.



**Equation for obtaining the initial cell count and final cell count outside the hydrogel:**

$$\frac{\text{Average Number of Cells in All Small Squares}}{0.00025 \mu\text{L}} = \frac{X}{5000 \mu\text{L}} * 3$$

The 0.00025 microliters (uL) represents the volume of each small square, the 5000 uL is the total amount of algae solution that was added to each hydrogel batch, and the 3 represents the  $\frac{1}{3}$  dilution made to the non-hydrogel samples. Lastly, the X is the total cell count in 5 mL of algae culture.

Example:

$$\frac{10.33 \text{ cells per small square}}{0.00025 \mu\text{L}} = \frac{6.20 \times 10^8 \text{ cells in 5 mL}}{5000 \mu\text{L}} * 3$$

**Equation for counting cells grown in hydrogel:**

$$\frac{\text{Total Mass of Hydrogel Batch}}{10 \text{ g removed}} = \alpha \quad \frac{300 \text{ mL of water}}{10 \text{ g hydrogel}} = \beta$$

$$\frac{\text{Average Number of Cells in All Medium Squares}}{0.004 \mu\text{L}} = \frac{X}{5000 \mu\text{L}} * \alpha * \beta$$

The 0.004 uL represents the volume of each medium square, the 5000 uL is the total amount of algae solution that was added to each hydrogel batch, and the  $\alpha$  and  $\beta$  represent the dilutions made by adding 10 g of hydrogel to 300 mL of water. Lastly, the X is the total cell count in 5 mL of algae culture separated from the hydrogel.

Example:

$$\frac{130.54 \text{ g}}{10 \text{ g removed}} = 13.054 \quad \frac{300 \text{ mL of water}}{10 \text{ g hydrogel}} = 30$$

$$\frac{6.2 \text{ cells per medium square}}{0.004 \mu\text{L}} = \frac{3.04 \times 10^9}{5000 \mu\text{L}} * 13.054 * 30$$

### 3D Bioprinting Methods

#### Modifying a Desktop 3D Printer for Extrusion of Hydrogels

A desktop thermoplastic 3D printer was modified to extrude hydrogel through 10 mL syringes. In 2019, Parsons and Caroway created a pneumatic extrusion system using an air compressor, flow regulator and solenoid valve. This system was able to deliver sufficient pressure for extruding a viscous fluid through luer lock syringe needles. However, the degree of pressure control available through the flow regulator was not accurate enough to provide steady and reliable extrusion. For this reason, the system was upgraded to accommodate proportional solenoid valves for finer pressure control, pressure transducers to precisely measure pressure, and a Raspberry Pi single board computer to monitor and control the air pressure.

Whenever hydrogel is extruded from a syringe, there are three variables dictating print quality: temperature, which affects viscosity; extrusion pressure; and print speed. Since 3D printing with viscous fluids is a relatively new technology, few have been able to precisely manipulate all three. Although in 2016, Suntornnond et al. developed a basic equation relating viscosity, pressure and extrusion width:

$$\Delta P = 32\eta L \cdot \left(\frac{3n+1}{4n}\right) \cdot \frac{d^2}{D^4} \cdot v$$

**Figure 6**  $\Delta P$ = net air pressure between atmosphere and syringe

$\eta$  = absolute viscosity of solution

$L$  = length of printing needle

$n$  = apparent viscosity of solution

$d$  = printed material width

$D$  = diameter of printing needle

$v$  = print head velocity

The goal of the pneumatic printing device in this study was to measure properties such as pressure  $\Delta P$  or viscosity  $\eta$  so that the mathematical model of this equation could be verified and the physical properties of carrageenan hydrogel could be validated. While viscosity was charted for each batch of gel, the data was largely unusable for printing because it constantly changed with respect to temperature. Due to a lack of temperature sensors on the printer, temperature and viscosity data *was not* used during the 3D printing process. Instead, the variable manipulated in this research was pressure. *For more details on the construction and programming of the upgraded pneumatic system see the supplementary materials at the end of this paper.*

### Determining Bioprinting Capabilities with a Hydrogel Line Test

After building the new bioprinting system, a line test was prepared to test the printing properties of the hydrogel as well as the capabilities of the 3D printer. This involved the printing of several hydrogel line segments. Using the 3D modelling program Autodesk Maya in combination with Slic3r, a commonly used Gcode slicer, a basic tool path was programmed to

test the hydrogel.

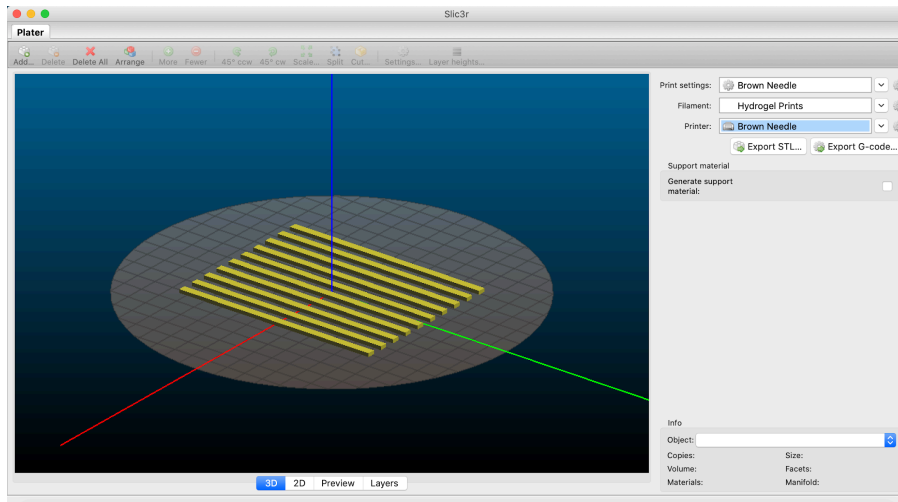


**Figure 7** 3D model loaded into Slic3r for conversion to Gcode

After preparing all the software elements, small acetate plastic circles were taped to the print bed for later removal and observation of hydrogel structures. During the line test, several different sizes of luer lock needle were tested to determine the most optimum extrusion diameter for hydrogel. The needle diameters were: 260, 340, 410, 510, and 840 micrometers ( $\mu\text{m}$ ). The first needle was attached, then the print was started. After one line was complete, the print was stopped and a new needle applied. This process was repeated for each needle size.

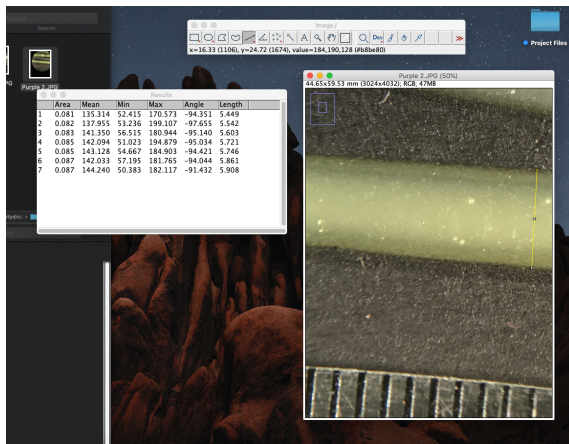


**Figure 8** *Algae laden hydrogel line in ImageJ*

For each sample, the plastic circle was removed from the printer and placed under an optical microscope for analysis. At  $\sim 7.5\times$  zoom, a ruler with millimeter markings was placed on top of the line segments. Pictures of the enlarged hydrogel were taken using a camcorder and television attached to

the microscope. These images were then imported into *ImageJ* and measured using built-in scale tools. Millimeter markings were recorded in the program as a number of pixels on the image, which were used to calculate printed hydrogel line widths. All of the samples were measured 20 times, in different places, to derive an average estimated width for each needle size.

## Hydrogel Results

### Results from Viscosity Test

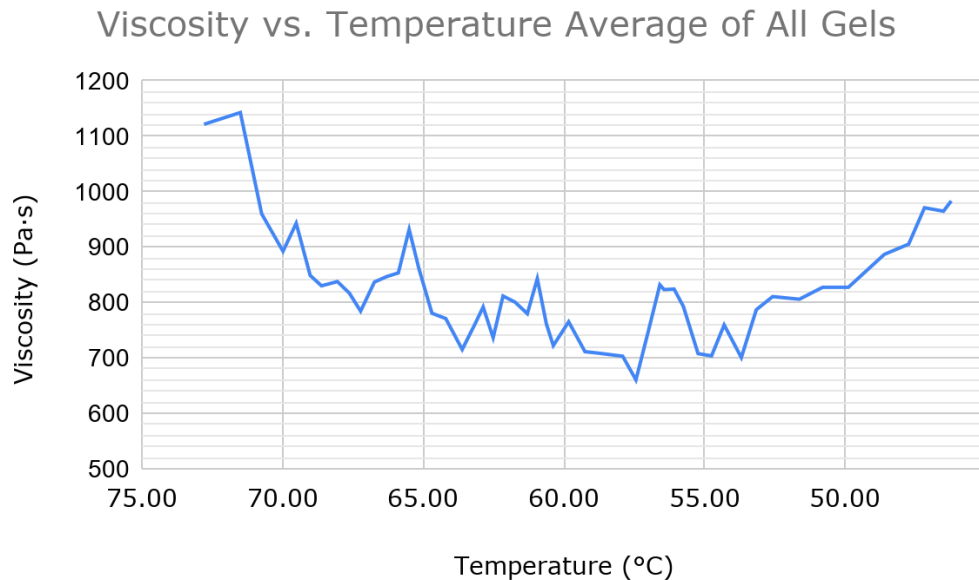


**Figure 9** “All Gels” refers to 18 batches of gel made on 11/21/19, 11/22, 11/25, 11/26, 12/2, and 12/4. Three batches were made per day. The goal of this data was to find an overall correlation of viscosity and temperature for carrageenan hydrogel. Due to an enormous spread in the data points, a moving average (subset of 4 was used) made it easier to visually represent such an immensely populated graph. While it was expected that individual solutions would naturally deviate from the overall viscosity-temperature relationship, the data was more spread out than anticipated. Since the cooling process was not controlled (the beakers were placed on a room temperature lab table), the temperature of the mixtures was lowered at varying rates. When viscosity data is implemented directly in the printing process, a close analysis of the temperature gradient throughout the hydrogel gel solution could be a better printability metric than rotational viscometry.

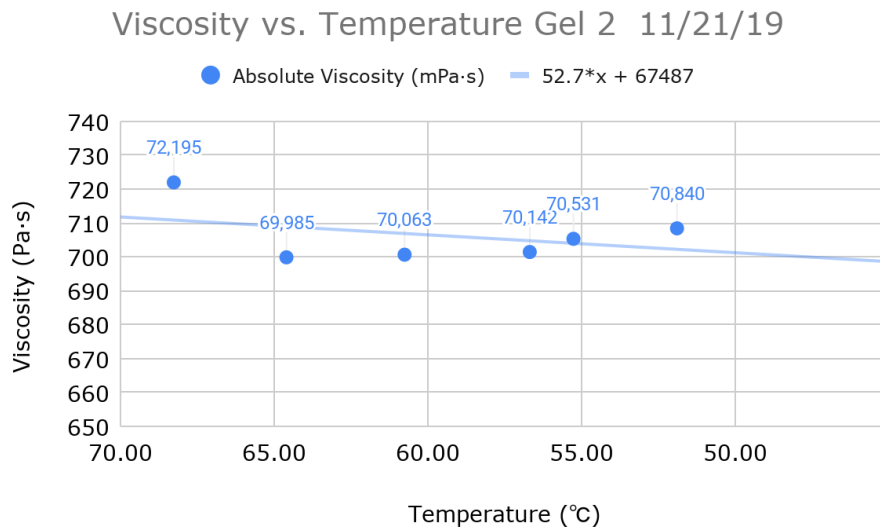
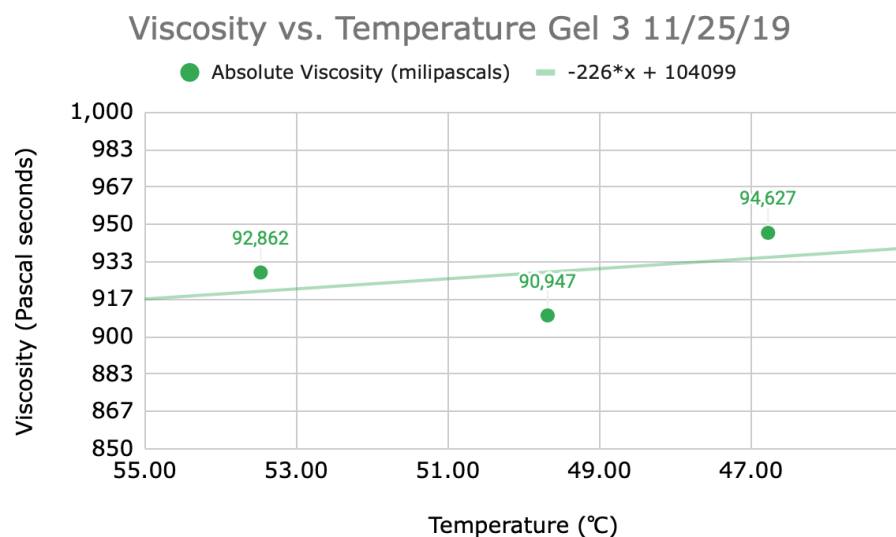
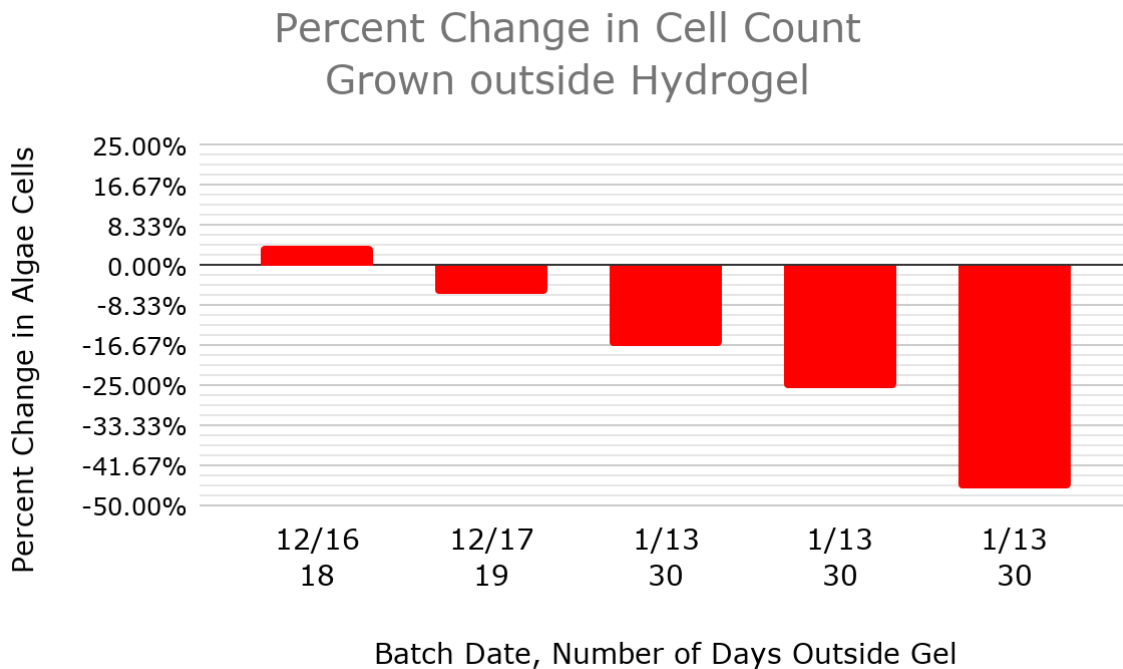


**Figure 10** shows the viscosity-temperature relationship of a specific hydrogel batch. This particular data set was the most representative of the combined graph, showing that the viscosity started out high, dropped suddenly, and then slowly increased. The time axis of this data was not included so the comparison between temperature and viscosity could be made, however during further research into the cooling rate of hydrogel, a degrees per second axis will be added to make data comparison easier. **Figure 11** shows a batch with a more positive viscosity-temperature relationship.



## Algae Results

### Results of Algae Cell Count



The x-axis of **Figure 12** shows the date each algal sample was taken for the original culture (December 2019, January 2020), followed by the number of days the algae was grown in microcentrifuge tubes. When not inserted in the hydrogel, little to no growth was observed. Also, negative percentages were calculated across many of the samples. This was caused by chlorophyll degradation, which made cell counting difficult due to a loss of contrast between the green algal cells and culture solution. With constant exposure to grow lights, the cell count likely increased rapidly and then immediately declined once there was less space to carry out photosynthesis, causing the cells to disintegrate along with their chlorophyll.

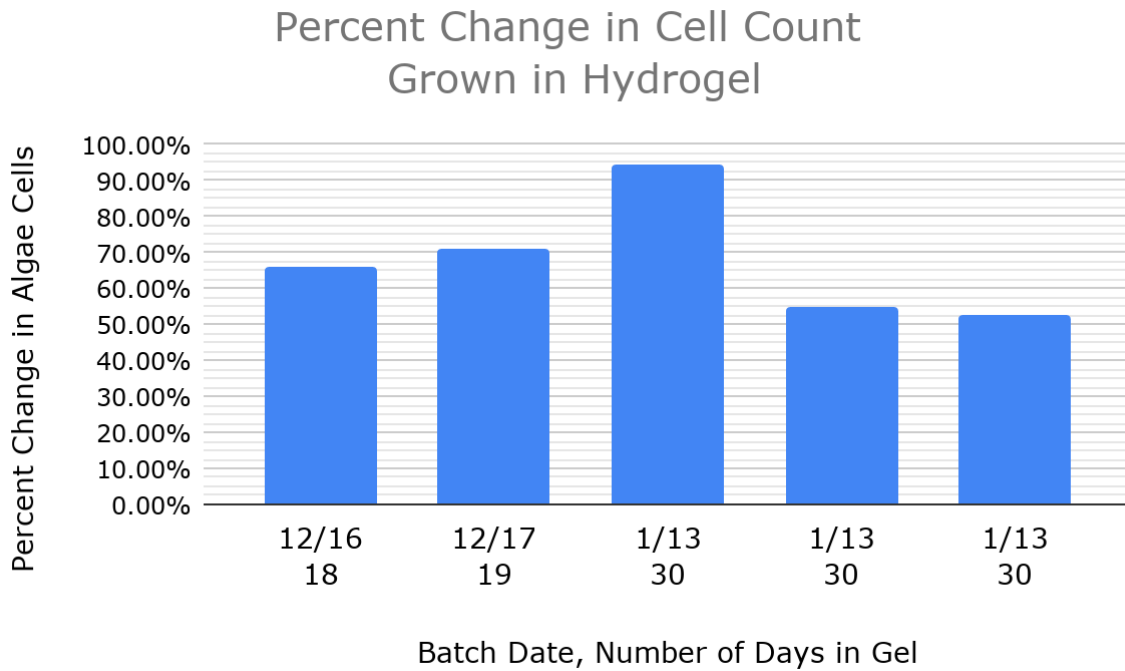


**Figure 13** displays the percent change in cell count for algae grown in hydrogel. These samples showed significant growth, reaching upwards of 94% of the original culture. **Figure 14** is a portion of the raw data from the cell counts of the batch that approached 94% growth. The chart labeled in green at the top of the figure is the cell counts of each small square recorded by three different people. The yellow chart shows the small square counts of the algae left to grow in the centrifuge tubes and the chart labeled in blue lists the number of cells in each medium square from counting the algae-laden hydrogel. **Figure 14:**

Initial Cell Count	Up Left	Bottom Left	Up Right	Bottom Right	Total		
Person 1	10	14	14	12	50	15.25	Average
Person 2	16	22	19	15	72	9.15E+08	Total in 5 mL
Person 3	14	14	15	18	61		
Final Cell Count	Up Left	Bottom Left	Up Right	Bottom Right	Total		
Person 1	7	12	17	14	50	12.66666667	Average
Person 2	9	13	13	14	49	7.60E+08	Total in 5 mL
Person 3	8	10	20	15	53		
Hydrogel Count	1T	2T	3T	4T	5T	1S	2S
Person 1	4	1	10	0	8	6	2
Person 2	1	6	0	1	4	2	2
Person 3	4	0	15	3	0	8	5
T = Top Row							
S = Second Row							

### 3D Bioprinting Results

#### Results from Hydrogel Line Test

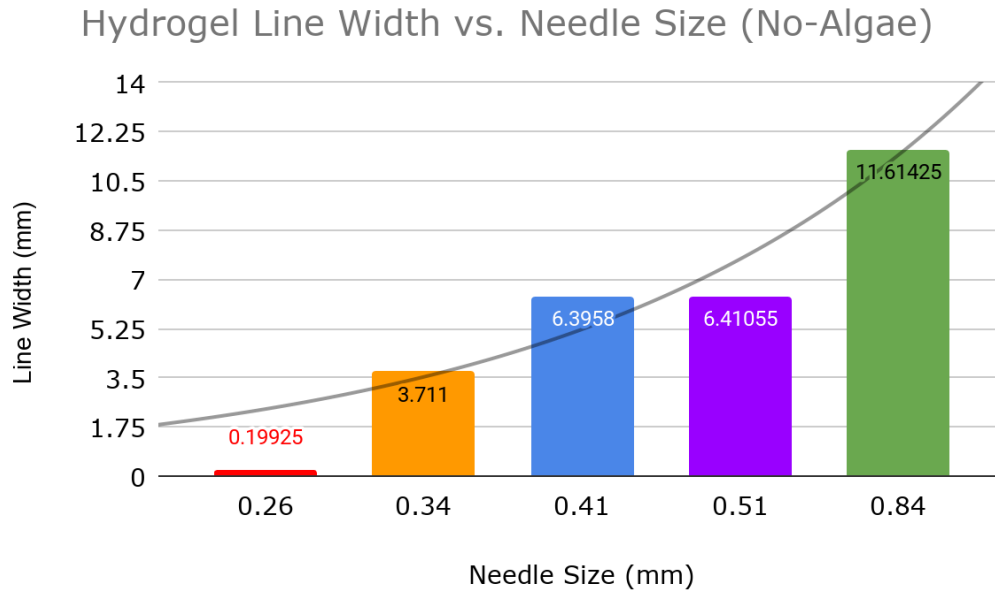


**Figure 15** shows the width of each printed line against the needle size (diameter) it was printed with. These 5 needle tests were done with algae-free hydrogel. While it appears that the relationship between needle size and extrusion is exponential, experimentation with more incremental sizes would show that the printed width increases proportionally. For example, the diameter range between 0.84 and 0.51 mm is greater than 0.51 and 0.41 mm, which accounts for the much wider printed width from the green needle (0.84 mm). Inconsistent movement of hydrogel within the needles also played a role in their major extrusion differences. With the red needle (0.26 mm) for instance, pressure being applied above the hydrogel was unable to accurately move material through the needle bore. This led to cooled hydrogel getting stuck in the hub of the needle, preventing further extrusion.

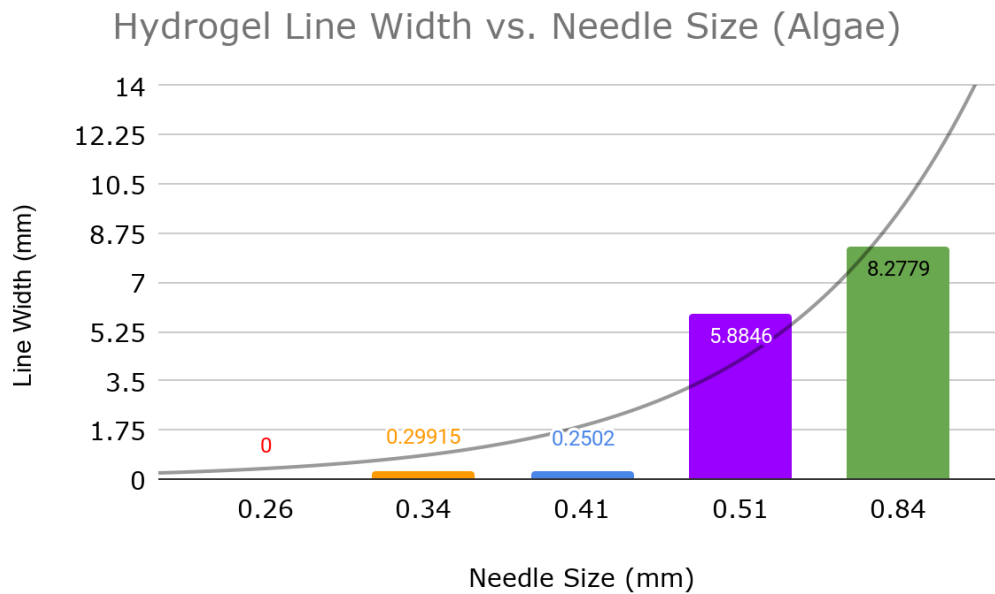


**Figure 16** shows the printed line widths for algae-infused hydrogel. The introduction of algae to hydrogel at a lower temperature (40°C) caused the material to gel and become much too viscous for printing. With needle diameters of 0.26, 0.35, and 0.41 mm, an insignificant amount of hydrogel was extruded. The purple and green needles, however, were still printable even at a decreased temperature.

All extrusion of hydrogel was done at room temperature, which made the process unpredictable because of uneven cooling in the material. In the case of the algae hydrogel, it was already too cool by the time the printer reached the print bed. If the temperature were maintained at 40°C, then the purple or green needles could be used more consistently.

## **Discussion**

### Hydrogel Discussion

Observing the consistency and structural properties of carrageenan hydrogel was crucial in determining its viability as a biofilter material. With available instruments, two important qualities of the highly viscous fluid were assessed: temperature and viscosity. Overall, the thermal characteristics were confidently reported with reasonable accuracy, demonstrating the most efficient way of heating and mixing hydrogel. In terms of viscosity, several factors were influencing the position of the viscometer's spindle. The first involved the leveling of the viscometer. While a small level was included on top of the viscometer housing, the device offered no additional method of calibration to the work surface beyond manually adjusting its stand. The other factor affecting spindle position was evaporation. After placing each beaker of hydrogel in the viscometer, the two left on the hotplate had more time to evaporate, and thus lost more volume. When the spindle was lowered into beakers of lesser volume, the hydrogel did not reach the minimum acceptable fluid line marked on the viscometer spindle. While only a few of the samples experienced this level of volume loss, it was extremely difficult to regulate the position of the spindle within each mixture. In addition to evaporation, as the hydrogel cooled it began to solidify, which should have increased the viscosity. However, in data from figure 12 a significant drop in the viscosity occurred from ~73 to 54°C. This was likely due to the hydrogel forming a slippery film on its surface, causing the spindle to rotate freely instead of being affected by the actual consistency of the solution.

### Algae Discussion

Counting cells with a chip hemocytometer was a novel way of quantifying algal growth. Previous hydrogel research by Malik et al. (2019) measured the growth of algae using photos taken after several days in the experiment. Through this method, they were able to qualitatively determine when the algae died using the shift in its green hue. While visual assessment is helpful in deducing the overall health of algae, actual counting of the cells can provide more detailed information about whether they reproduce or immediately die off.

By using the chip method, it was observed that the algae did grow considerably while in the hydrogel. The control algae cultures, which were grown separately from the hydrogel in low volume microcentrifuge tubes, showed negative growth. This was most likely from dead cells disintegrate in the solution. The low volume microcentrifuge tubes drastically limited available nutrients and surface area for the control organisms to grow in. This questions the validity of the control data. A more fair comparison between the hydrogel and non-hydrogel samples would be to grow 5 mL of liquid culture alongside the 5 mL of algae added to each hydrogel batch.

One issue with quantifying the cells was human error in counting the grid. Even more people to count each sample would help to further reduce bias. Also, using computer software to automatically count cells could potentially speed up the process.

### 3D Bioprinting Discussion

Hydrogel, as a printable material, is versatile due to thermal-reversibility and tensile strength, however it suffers from multiple drawbacks. When *Chlorella Vulgaris* is inserted into the hydrogel, in order for the algae to live, it needs to remain below a temperature threshold. Hydrogel begins to harden as it cools, which forces precise timing to occur when printing hydrogel containing algae. Because of this, variation in hydrogel temperatures can make a major difference in print quality or algae lifespan.

The data revealed through these line tests shows that large needle diameters may have to be used when printing cooler hydrogel. In the line test with algae added, a noticeable shift in the graph occurs. Smaller needle sizes that would have extruded well with no algae fail to do so with algae introduced. This is most likely due to the increased cooling effect caused from adding the algae with its liquid culture solution. The algae could have also reduced the homogeneity of the solution by cooling certain parts and leaving others still a warm fluid. This creates chunks of hydrogel which can get stuck in the bore of printing needles. One needle size that remained consistent throughout these line tests was purple (510  $\mu\text{m}$ ). This middle size offered a reasonable balance between high print resolution and extrudability of cooled gel.

## Conclusion

Photosynthetic algae *Chlorella Vulgaris* was successfully grown in carrageenan hydrogel. This was accomplished without the aid of additional nutrients. It grew for roughly 20 days with only the water present in the gel and the carrageenan as a source of nutrients. Also, this particular hydrogel formulation of carrageenan and nanosilicates had never been tested previously with algae. In addition to successfully growing algae, a new method for quantifying algal growth was employed using a chip hemocytometer. Monitoring the health of organisms inside hydrogel can be difficult as the cells are not easily accessible. While accurate, real time monitoring systems for cell growth inside hydrogel are not currently possible, this research shows that small amounts of the gel can be removed and tested accurately. In an industrial scale hydrogel membrane, removal of 10 g would be quite minimal.

The 3D bioprinter system was drastically improved through the use of proportional solenoid valves. This allowed for fine adjustment of air pressure, making it easier to print hydrogel with a changing viscosity. Despite needing a larger needle size, algae laden hydrogel was extruded in basic line structures using a custom Gcode toolpath. This showed that carrageenan hydrogel is a promising option for additive manufacturing because of its ability to cool quickly and retain a rigid structure. It also showed that printing hydrogel at a temperature appropriate for algae is still possible despite the gel beginning to harden.

## Future Work

Despite the versatility and low cost of hydrogel, there is little research put into optimizing this compound for printing and practical use. In order for hydrogel—and the algae it contains—to function at an optimal level, testing of numerous hydrogel formulations is required. Prior studies have shown that hydrogel can be improved by modifying the material concentrations and crosslinking temperatures (Wilson et al, 2017), which could prove beneficial, however research is limited. Further testing would likely result in cheaper and more effective hydrogel. In addition to optimizing the hydrogel itself, working to obtain more viscosity and temperature data could help in automating the print process. This would reduce human error, resulting in more precise and complex hydrogel structures.

In terms of algal growth, the thermal tolerance of *Chlorella Vulgaris* should be further investigated. If it can withstand greater temperatures than the currently recommended range (0-37°C), then the hydrogel could be printed at a higher temperature. The effects of hydrogel on *Chlorella Vulgaris* were investigated in this study, however other algae species could be experimented with, proving more insight into the properties of hydrogel and its effect on microorganisms.

## References

- Calvert, P. (2016). 3d printing of gels with living photosynthetic algae. *Materials Research Society*. doi:10.1557/adv.2016.455
- Caroline Burgess Clifford. (n.d.). 10.3 Algae Growth and Reaction Conditions. Retrieved from <https://www.e-education.psu.edu/egee439/node/694>
- Devlinny, J. S., Deshusses, M. A., & Webster, T. S. (1998). *Biofiltration for Air Pollution Control*. Boca Raton, FL: CRC Press.
- Environmental Protection Agency. (2002). Air Pollution Control Technology Fact Sheet. Retrieved from <https://www3.epa.gov/ttnca1/dir1/ffdg.pdf>
- Environmental Protection Agency. (2019, August 28). Managing Air Quality - Control Strategies to Achieve Air Pollution Reduction. Retrieved from <https://www.epa.gov/air-quality-management-process/managing-air-quality-control-strategies-achieve-air-pollution>
- Gonzalez-Delgado, A. D., Barajas-Solano, A. F., & Peralta-Ruiz, Y. Y. (2016). Microalgae immobilization using hydrogels for environmental applications: study of transient photopolymerization. *Chemical Engineering Transactions*, 47. doi:10.3303/CET1647077
- IGV GmbH. (2011, September 28). Photobioreactor Design Principles, Submariner Project Cooperation Event: Present and Potential Uses of Algae. Retrieved from <http://>

[www.submariner-project.eu/images/stories/events/algae-trelleborg/presentations/wencker.pdf](http://www.submariner-project.eu/images/stories/events/algae-trelleborg/presentations/wencker.pdf)

International Energy Agency. (2019). Global Energy & CO2 Status Report: CO2 emissions.

Retrieved from <https://www.iea.org/geco/emissions/>

Jovic, T. H., Kungwengwe, G., Mills, A. C., & Whitaker, I. S. (2019). Plant-Derived

Biomaterials: A Review of 3D Bioprinting and Biomedical Applications. *Frontiers in Mechanical Engineering*, 5(19). doi:10.3389/fmech.2019.00019

Malik, S., Hagopian, J., Mohite, S., Lintong, C., Stoffels, L., Giannakopoulos, S., ... Parker, B.

(2019). Robotic Extrusion of Algae-Laden Hydrogels for Large-Scale Applications. *Global Challenges*, 4(1), 1900064. doi:10.1002/gch2.201900064

NASA. (2010, December 9). World of Change: Global Temperatures. Retrieved from [https://](https://earthobservatory.nasa.gov/world-of-change/DecadalTemp)

[earthobservatory.nasa.gov/world-of-change/DecadalTemp](https://earthobservatory.nasa.gov/world-of-change/DecadalTemp)

National Cooperative Extension. (2019, April 3). Algae for Biofuel Production. Retrieved from

<https://farm-energy.extension.org/algae-for-biofuel-production/>

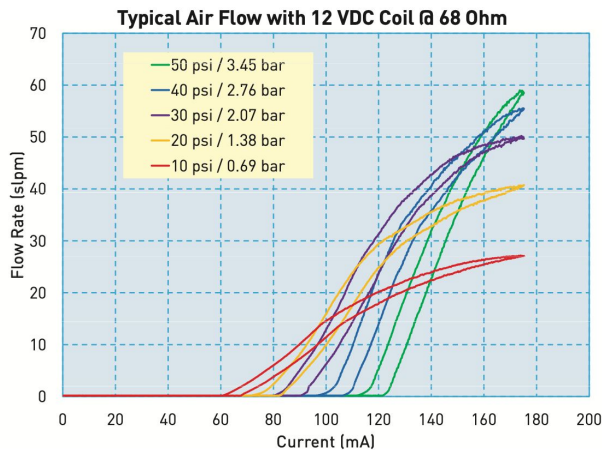
NOAA. (2019). Climate Change: Atmospheric Carbon Dioxide. Retrieved from [https://](https://www.climate.gov/news-features/understanding-climate/climate-change-atmospheric-carbon-dioxide)

[www.climate.gov/news-features/understanding-climate/climate-change-atmospheric-carbon-dioxide](https://www.climate.gov/news-features/understanding-climate/climate-change-atmospheric-carbon-dioxide)

- Schaffner, M., Ruhs, P. A., Coulter, F., Kilcher, S., & Stuart, A. R. (2017). 3d printing of bacteria into functional complex materials. *Science Advances*, 3(12). doi:10.1126/sciadv.aao6804
- Suntornnond, R., Tan, E. Y., An, J., & Chua, C. K. (2016). A mathematical model on the resolution of extrusion bioprinting for the development of new bioinks. *Materials*, 9(756). doi:10.3390/ma9090756
- U.S. Department of Energy. (2012). Algal Biofuels. Retrieved from <https://www.energy.gov/eere/bioenergy/algal-biofuels>
- University of Kentucky. (2013, September 27). *Algae CO2 Capture at the University of Kentucky: Part 1* [Video file]. Retrieved from <https://www.youtube.com/watch?v=QI3A11dpuUY>
- Wilson, S. A., Cross, L. M., Peak, C. W., & Gaharwar, A. K. (n.d.). Shear-thinning an thermo-reversible nano engineered inks for 3D bioprinting. *ACS Applied Materials and Interfaces*, 9. doi:10.1021/acsami.7b13602
- Yokpradit, A., Tongloy, T., Kaewpirom, S., & Boonsang, S. (2018). A real-time rheological measurement for biopolymer 3d printing process. *Sensors and Materials*, 30(10). doi:10.18494/SAM.2018.1851

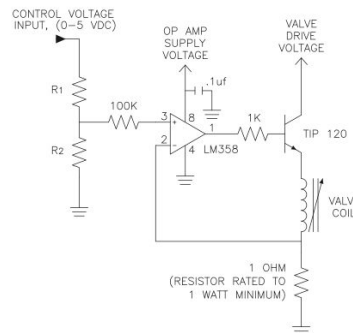
## Supplementary Materials: 3D Printer Diagrams, Schematics and Code

- ❑ To properly control the two solenoid valves, a custom circuit was designed to provide *constant voltage* and *variable current* for each valve.
- ❑ We used recommendations from the manufacturer's datasheet to determine optimal circuit layout and power requirements:  
[http://aldax.se/wp-content/uploads/2012/12/HFPRO-9\\_26\\_12.pdf](http://aldax.se/wp-content/uploads/2012/12/HFPRO-9_26_12.pdf)
- ❑ In this diagram, they show a relationship between airflow and current. These are 12 volt (v) devices that are most sensitive in a range of 80 to 180 milliamps (mA):



- ❑ Since our goal was to control the valves with a variable *voltage* instead of current, a circuit that could take a weaker 0 to 5v signal from a microcontroller (such as arduino or raspberry) and convert it to a steady 12v with low current was needed. Luckily the datasheet also provided an outline of how to achieve this:

### Suggested HF PRO Current Driver Schematic



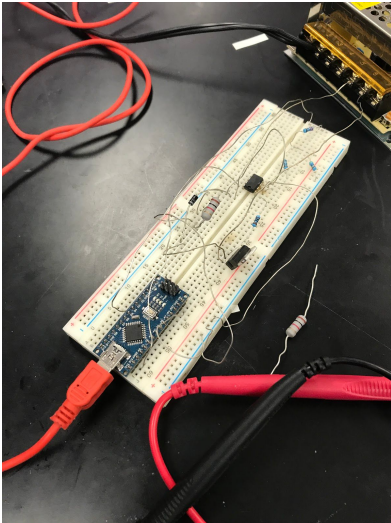
This simple current driver circuit draws only 1 mA at the input control (0-5VDC) and provides control for any HF PRO configuration regardless of valve voltage or resistance.

Table 3 (below) describes the recommended R1 and R2 resistor values based upon the full shut-off current.

**Table 3: Selectable Resistor Values for a Low Current (1mA) LM358-Based Current Driver**

Voltage Supplied to Valve Coil [Reference]	Valve Drive Voltage [VDC]	Nominal Coil Resistance @ 20°C [Ohms]	Input Current for Full Flow [mA]	R1 [Ohms]	R2 [Ohms]
5	7	11.9	435	1000	95.3
12	14	68	175	2260	33.6
24	26	274	87	4990	18.2

- Once we ordered all the components necessary to begin assembly of the circuit, we started to prototype everything on a breadboard:



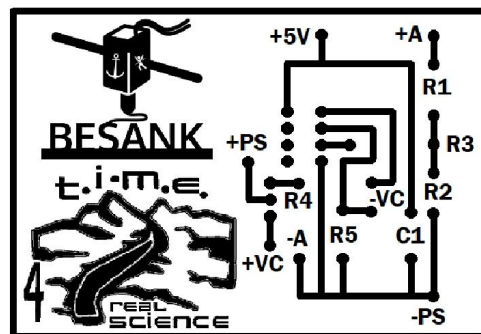
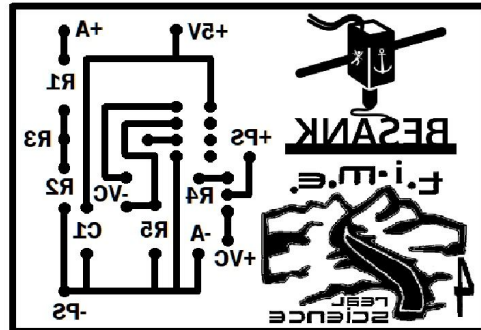
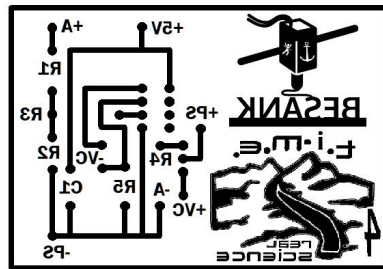
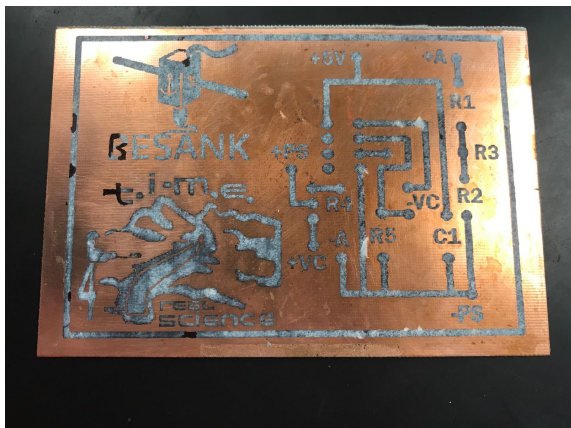
- After everything functioned correctly with our Arduino microcontroller, we moved on to designing a more permanent installation for the circuit.

- First, using the manufacturer's diagram, a printable template was drawn in Microsoft Paint.

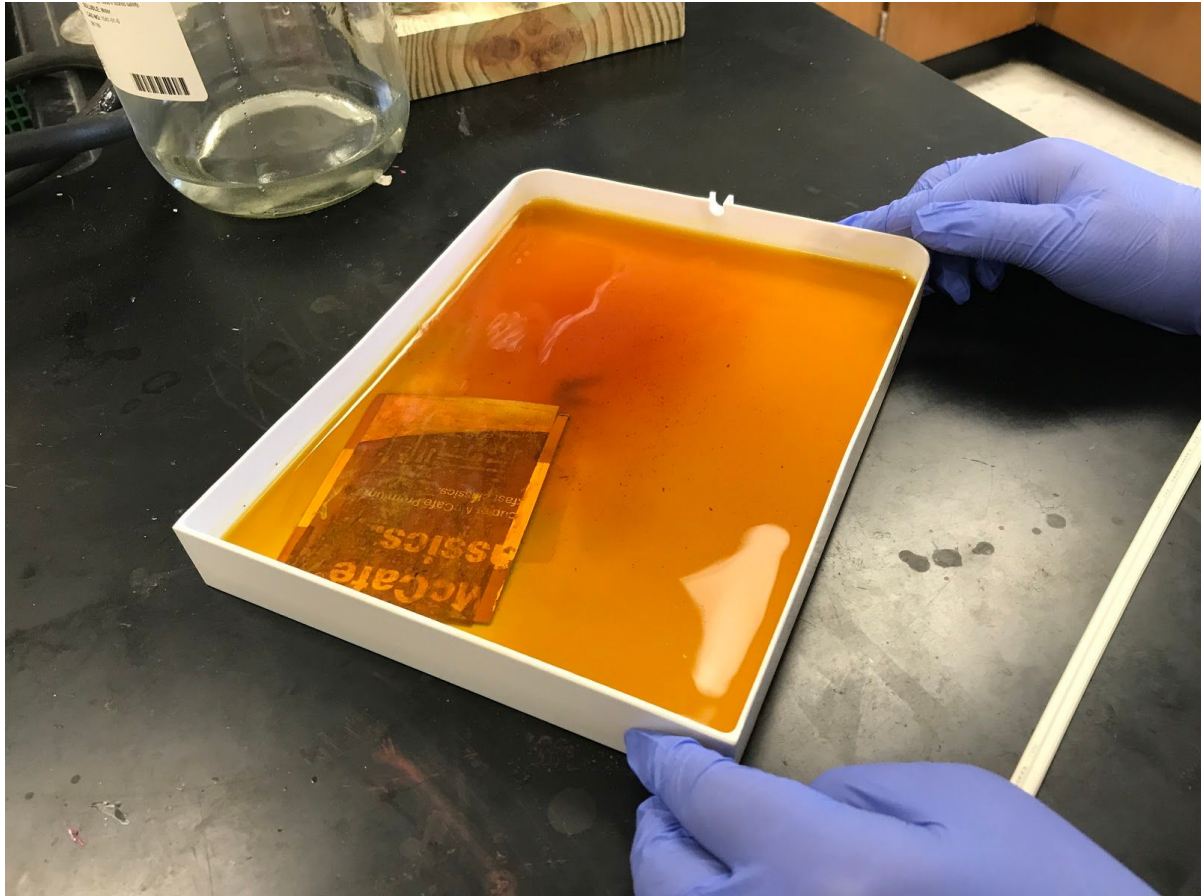
- All the resistor values and components were labeled, along with holes for leads and traces to be etched:

- After creating our circuit design, it was printed in a flipped orientation so that when it was placed face down on the copper perf board traces and holes would face up the correct way.

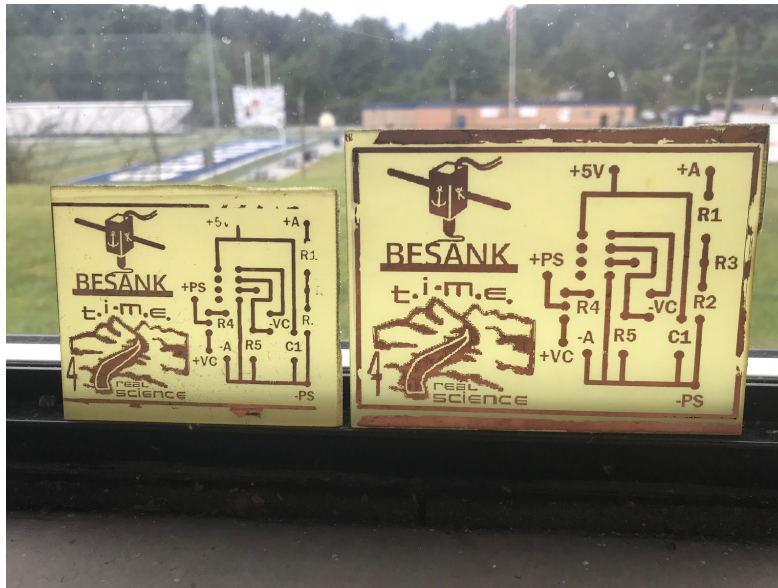
- The layout was printed on glossy magazine paper to ensure maximum adhesion to the copper board when ironed:



- ❑ Once the ink for the design had thoroughly adhered to the copper board, a solution of ferric chloride was used to etch away excess copper:

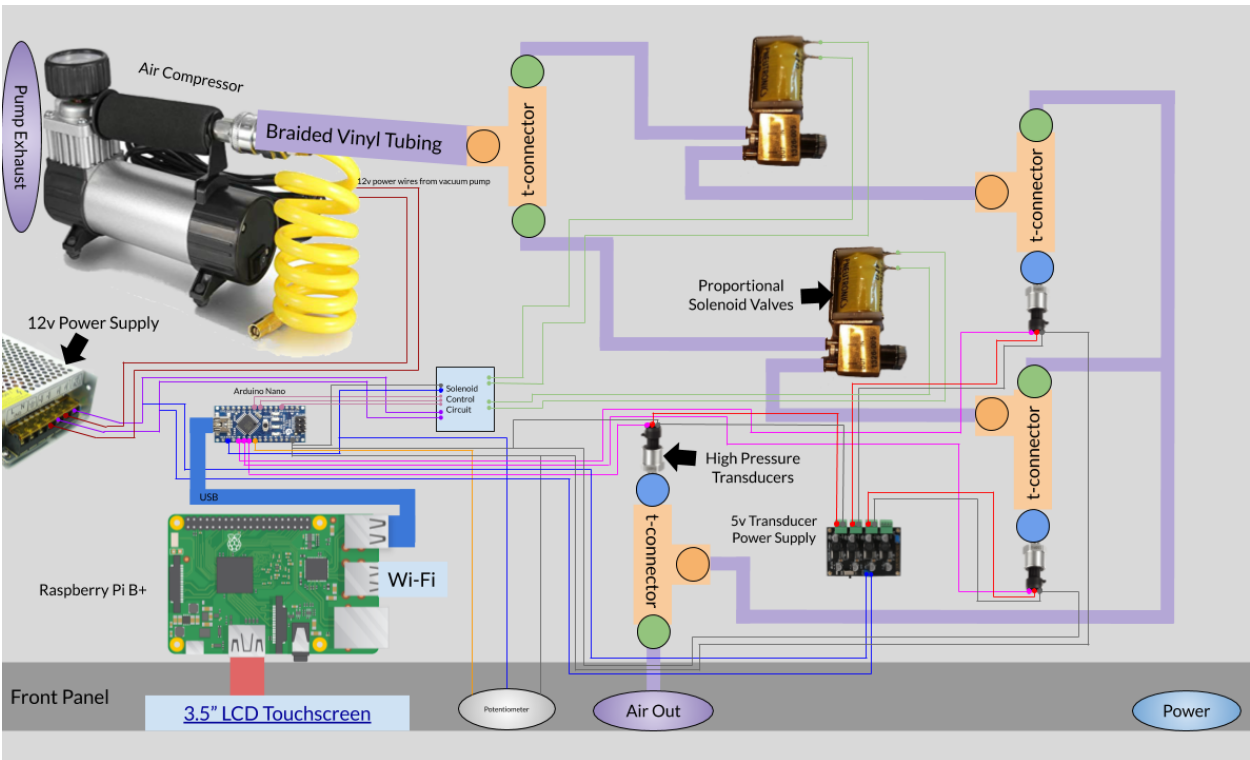


- ❑ Later on, we ended up using 1 M hydrochloric acid which was much faster and produced a much cleaner board.
- ❑ The final circuit with soldered components:

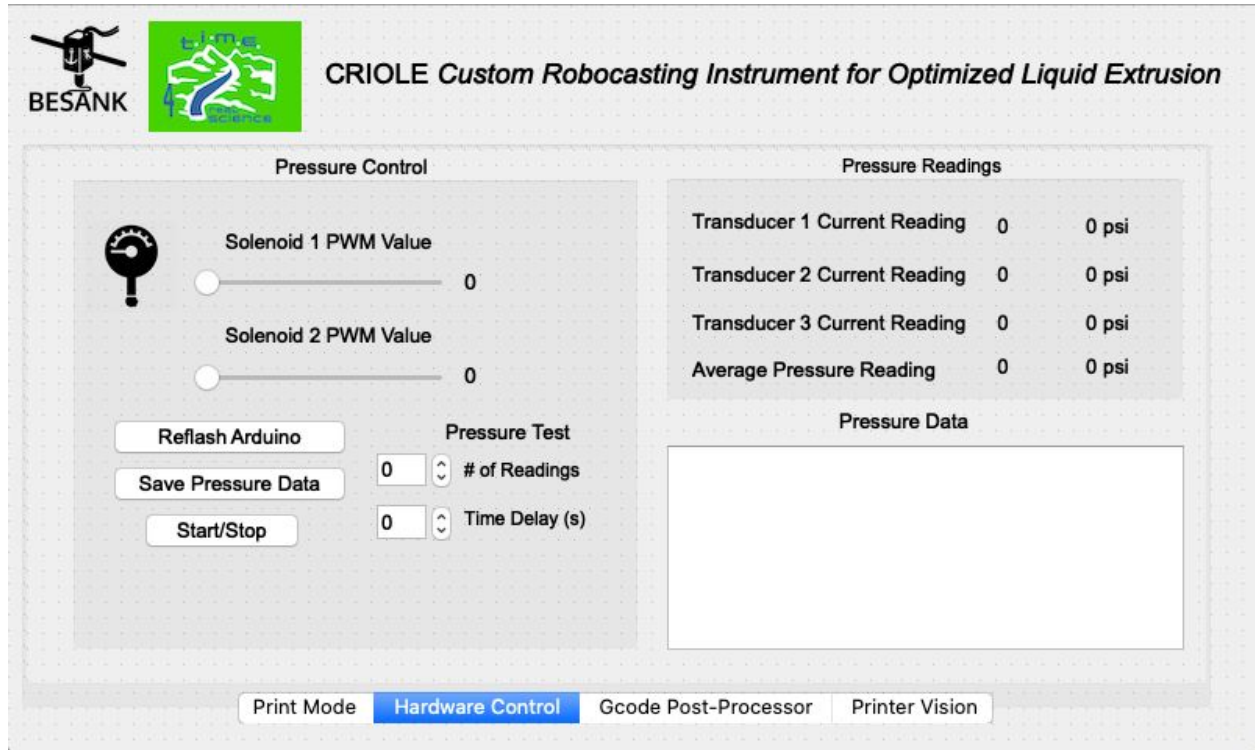


## Code and Final Robocasting Device

- ❑ After creation of solenoid valve control circuits, a final pneumatic pump was constructed to adjust airflow for the hydrogel extruder.
- ❑ The basic components of the pump include: a Raspberry Pi computer, Arduino microcontroller, two solenoid valves, 3 pressure transducers, an lcd screen, tubing, wiring and power supplies:



- ❑ The pressure transducers are not utilized in the current product. We were limited by time constraints and unable to complete our code.
- ❑ A basic graphical user interface (GUI) was programmed in QT Creator to provide an ease of interaction with the system.
- ❑ Simple, draggable sliders were added to the interface to send pulse width modulation (PWM) signals to the Arduino, which then controlled the voltage of each circuit.
- ❑ An image of the GUI on the next page shows the sliders as well as additional features that have yet to become functional



- ❑ The Custom Robocasting Instrument for Optimized Liquid Extrusion or CRIOLE for short, is the official term we used for our pneumatic pump.
  
- ❑ Listed below is the most recent version of our code that produces the GUI listed above and interacts with the solenoid valves via the Arduino:

```

1  from PyQt5 import QtCore, QtGui, QtWidgets
2  from PyQt5.QtWidgets import QMainWindow, QApplication, QWidget, QAction, QTableWidgetItem, QVBoxLayout
3  from CRIOLE_UI import Ui_CRIOLE
4  import sys
5  import os
6  import time
7  from nanpy import ArduinoApi, SerialManager
8  from time import sleep
9
10
11 class CRIOLE(Ui_CRIOLE):
12     def __init__(self, dialog):
13         Ui_CRIOLE.__init__(self)
14         self.setupUi(dialog)
15
16         zero = 0
17
18         self.solenoid1Input.setMinimum(240)
19         self.solenoid1Input.setMaximum(255)
20         self.solenoid1Input.setValue(240)
21         self.solenoid1Input.setTickInterval(1)
22
23         self.solenoid2Input.setMinimum(240)
24         self.solenoid2Input.setMaximum(255)
25         self.solenoid2Input.setValue(240)
26         self.solenoid2Input.setTickInterval(1)
27
28         self.solenoid1Input.valueChanged.connect(self.valuechange)
29         self.solenoid2Input.valueChanged.connect(self.valuechange)
30
31         self.reflashArduino.clicked.connect(self.connectArduino)
32
33         self.pressureData.setColumnCount(5)
34
35         self.startPressureTest.clicked.connect(self.readPressureData)
36
37
38     def readPressureData(self):
39         counter = self.pressureTestCounter.value()
40         timeDelay = self.timeDelay.value()
41         self.pressureData.setRowCount(counter + 1)
42
43         columnHeader1 = QTableWidgetItem("Reading #")
44         columnHeader2 = QTableWidgetItem("T1")
45         columnHeader3 = QTableWidgetItem("T2")
46         columnHeader4 = QTableWidgetItem("T3")
47         columnHeader5 = QTableWidgetItem("AVG")
48
49         self.pressureData.setItem(1,1, columnHeader1)
50         self.pressureData.setItem(1,2, columnHeader2)
51         self.pressureData.setItem(1,3, columnHeader3)
52         self.pressureData.setItem(1,4, columnHeader4)
53         self.pressureData.setItem(1,5, columnHeader5)
54         self.pressureData.show()
55
56
57         for x in range(counter):
58             transducer1Reading = a.analogRead(transducerPin1)
59             transducer2Reading = a.analogRead(transducerPin2)
60             transducer3Reading = a.analogRead(transducerPin3)
61
62             transducer1Modified = transducer1Reading * (5/1023)
63             transducer2Modified = transducer2Reading * (5/1023)
64             transducer3Modified = transducer3Reading * (5/1023)
65
66             self.transducer1Voltage.setText(str(transducer1Modified))
67             self.transducer2Voltage.setText(str(transducer2Modified))
68             self.transducer3Voltage.setText(str(transducer3Modified))
69
70             transducer1ModifiedPSI = (transducer1Reading * (5/1023))*37.5
71             transducer2ModifiedPSI = (transducer2Reading * (5/1023))*37.5
72             transducer3ModifiedPSI = (transducer3Reading * (5/1023))*37.5
73

```

```

74         self.transducer1PSI.setText(str(transducer1ModifiedPSI))
75         self.transducer2PSI.setText(str(transducer2ModifiedPSI))
76         self.transducer3PSI.setText(str(transducer3ModifiedPSI))
77
78         self.pressureData.setItem(x,1, QTableWidgetItem(str(x)))
79         self.pressureData.setItem(x,2, QTableWidgetItem(str(transducer1Modified)))
80         self.pressureData.setItem(x,3, QTableWidgetItem(str(transducer2Modified)))
81         self.pressureData.setItem(x,4, QTableWidgetItem(str(transducer3Modified)))
82         self.pressureData.setItem(x,5, QTableWidgetItem(str((transducer1Modified+transducer2Modified+transducer3Modified)/3)))
83         self.pressureData.show()
84
85         time.sleep(timeDelay)
86
87     def connectArduino(self):
88         solenoidPin1 = 5
89         solenoidPin2 = 6
90         transducerPin1 = 14
91         transducerPin2 = 15
92         transducerPin3 = 16
93
94         try:
95             connection = SerialManager(device = '/dev/ttyACM0')
96             a = ArduinoApi(connection = connection)
97         except:
98             print("Failed to connect to CRIOLE")
99
100         #Setting up solenoid outputs
101         a.pinMode(solenoidPin1, a.OUTPUT)
102         a.pinMode(solenoidPin2, a.OUTPUT)
103         a.pinMode(transducerPin1, a.INPUT)
104         a.pinMode(transducerPin2, a.INPUT)
105         a.pinMode(transducerPin3, a.INPUT)
106
107
108     def valuechange(self):
109         solenoid1CurrentValue = self.solenoid1Input.value()
110         solenoid2CurrentValue = self.solenoid2Input.value()
111
112         self.slider1Value.setText(str(solenoid1CurrentValue))
113         self.slider2Value.setText(str(solenoid2CurrentValue))
114
115         a.analogWrite(solenoidPin1, solenoid1CurrentValue)
116         a.analogWrite(solenoidPin2, solenoid2CurrentValue)
117
118
119 if __name__ == '__main__':
120     solenoidPin1 = 5
121     solenoidPin2 = 6
122     transducerPin1 = 14
123     transducerPin2 = 15
124     transducerPin3 = 16
125
126     try:
127         connection = SerialManager(device = '/dev/ttyACM0')
128         a = ArduinoApi(connection = connection)
129     except:
130         print("Failed to connect to CRIOLE")
131
132     #Setting up solenoid outputs
133     a.pinMode(solenoidPin1, a.OUTPUT)
134     a.pinMode(solenoidPin2, a.OUTPUT)
135     a.pinMode(transducerPin1, a.INPUT)
136     a.pinMode(transducerPin2, a.INPUT)
137     a.pinMode(transducerPin3, a.INPUT)
138
139     app = QtWidgets.QApplication(sys.argv)
140     dialog = QtWidgets.QDialog()
141     prog = CRIOLE(dialog)
142     dialog.show()
143     sys.exit(app.exec_())
144

```